Research Square

Preprints are preliminary reports that have not undergone peer review.
They should not be considered conclusive, used to inform clinical practice,
or referenced by the media as validated information.

Effect of Particle Size and Process Intensification Techniques on Cellulose Recovery from Groundnut Processing Industry Waste

SANTHOSH K
National Institute of Food Technology, Entrepreneurship, and Management
DASHELYA K
National Institute of Food Technology, Entrepreneurship, and Management
Pratibha Singh
National Institute of Food Technology Entrepreneurship and Management-Thanjavur
Vidyalakshmi R
National Institute of Food Technology Entrepreneurship and Management-Thanjavur
Sinija VR
sinija@iifpt.edu.in

National Institute of Food Technology, Entrepreneurship, and Management

Research Article

Keywords: Groundnut shell, particle size optimization, cellulose extraction, waste valorization, process intensification techniques

Posted Date: August 13th, 2026

DOI: https://doi.org/10.21203/rs.3.rs-9994124/v1

License: This work is licensed under a Creative Commons Attribution 4.0 International License.
Read Full License

Additional Declarations: No competing interests reported.

Version of Record: A version of this preprint was published at Biomass Conversion and Biorefinery on October 21st, 2026. See the published version at https://doi.org/10.1007/s13399-026-07321-5.

Effect of Particle Size and Process Intensification Techniques on Cellulose Recovery from Groundnut Processing Industry Waste

Santhosh K[1], Dashelya K[2], Pratibha Singh[3], R. Vidyalakshmi[4] and Sinija V.R[2*]

[1]Department of Food Process Technology
[2]Department of Food Process Engineering
[3]Department of Food Plant Operation, Incubation and Entrepreneurship
[4]Department of Food Safety and Quality Assurance

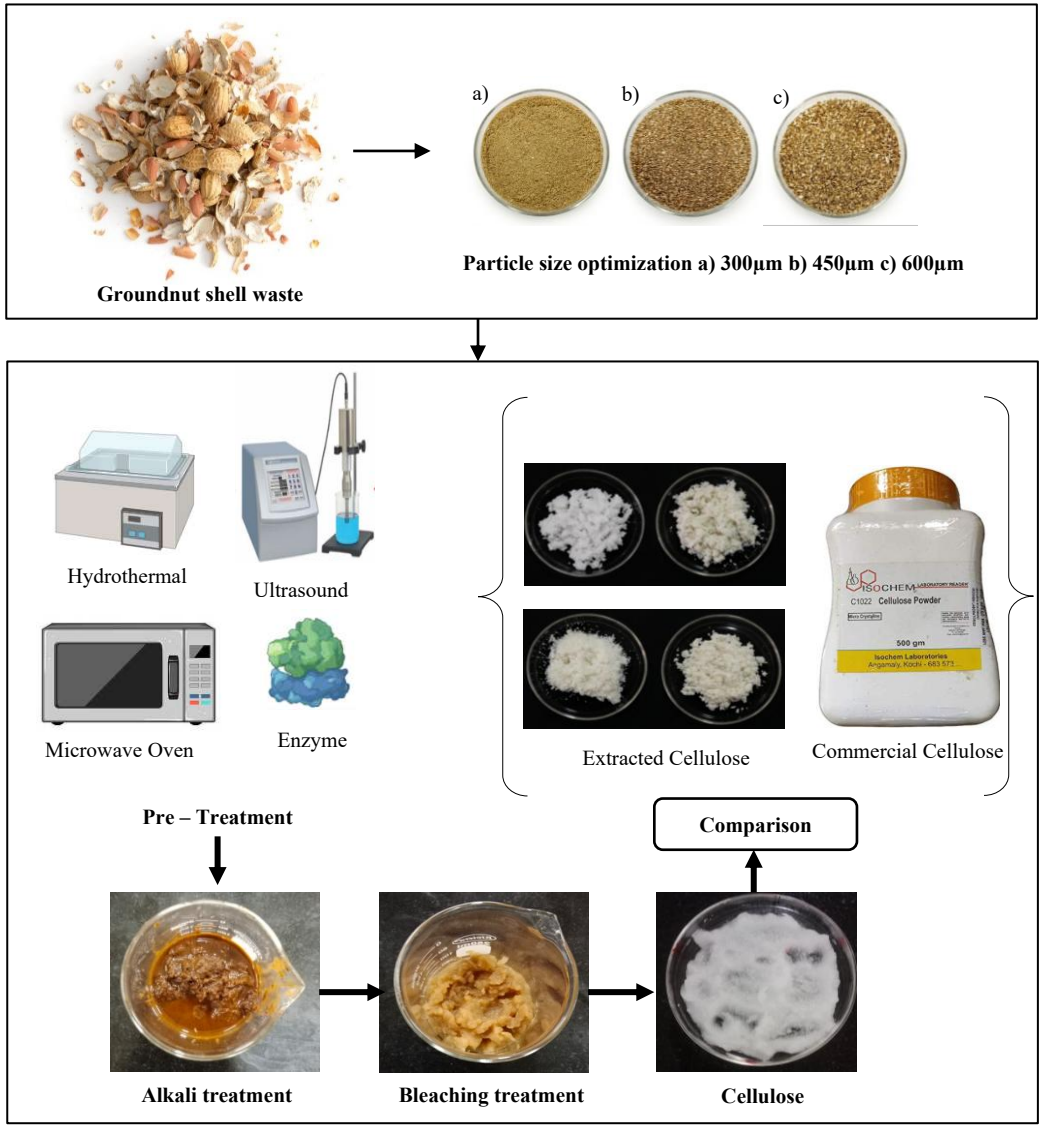
National Institute of Food Technology Entrepreneurship and Management – Thanjavur (NIFTEM-T), Tamil Nadu, India 613005.

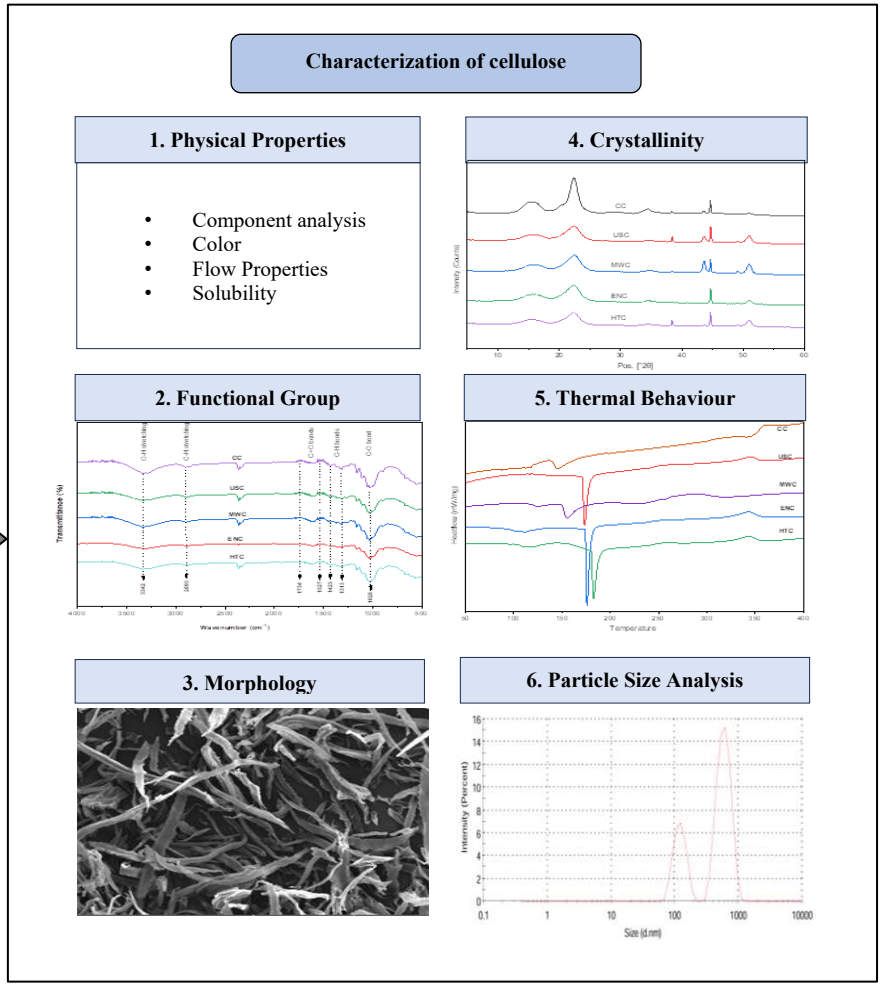
*Corresponding author Email: sinija@iifpt.edu.in

Abstract: The present study investigated, the effect of different process intensification techniques like, hydrothermal, microwave, ultrasound and enzyme pretreatments on extraction of cellulose from groundnut shell (GS). The extracted cellulose samples were compared with commercial cellulose (CC). Further, the impact of different particle sizes i.e., 300, 450 and 600 µm, on the extraction process has been analysed, and found that particle size of 450 µm showed better results. The cellulose yield ranged from 49.80 - 56.75%, indicating efficient removal of lignin and hemicellulose and enrichment of α-cellulose content. The structural analysis showed that the obtained cellulose had the same cellulose I crystalline structure, where the XRD peaks were found at 2θ = 22–23°. Also, the FTIR analysis showed that the samples had distinct O-H (3342 cm^{-1}) and C-H (2893 cm^{-1}) stretching vibrational peaks. The thermal analysis showed degradation between 280–360 °C, indicating high thermal stability due to increased crystallinity. The morphological analysis showed a change in morphology from compact structures to fibrous and porous structures after extraction. Particle size analysis showed that ultrasound treatment produced smaller and more refined cellulose particles compared to other treatments. The values for the lightness parameter (L*), which was close to commercial cellulose. Overall, the extracted cellulose exhibited physicochemical and structural properties comparable to CC. Among the pre-treatment, ultrasound was selected as the optimized extraction approach due to its improved cellulose purity and controlled delignification behaviour. This study demonstrated the potential of GS as a sustainable alternative source for high-quality cellulose production.

Key words; *Groundnut shell, particle size optimization, cellulose extraction, waste valorization, process intensification techniques*.

Graphical Abstract





1. Introduction

The rapid growth of the agricultural and food processing industries has resulted in the generation of lignocellulosic residues on a mass scale across the world. The uncontrolled generation of these agro-industrial residues has resulted in major environmental concerns such as greenhouse emissions, land pollution, and inefficient use of resources. The burning of these residues in open fields is a common practice in many countries, resulting in significant pollution of air and land [1]. These residues are a promising lignocellulosic biomass resource that can be utilized to produce high value-added bioproducts. The lignocellulosic biomass is a complex mixture of lignin, hemicelluloses, and celluloses in a recalcitrant matrix. Among these constituents, cellulose is the most abundant biomacromolecule on Earth and is the major structural component of plant cell walls [2]. The structural features of cellulose include linear chains of β-D-glucose units linked by 1,4-glycosidic bonds that form highly organized structures via hydrogen bonding [3]. Due to its renewability, biodegradability, non-toxicity, and versatility, cellulose has been widely employed in various food processing, pharmaceutical, textile, paper, packaging, and composite materials industries [4].

Traditionally, commercial cellulose is mainly derived from woody biomass, contributing to almost 90-95% of global cellulosic pulp production. Nevertheless, with an increase in sustainable and non-woody materials, agricultural wastes have emerged as potential materials for commercial cellulosic production [5]. Agricultural wastes have lower lignin content and high renewability, providing an advantage over woody biomass in commercial cellulosic production processes. Groundnut (*Arachis hypogaea* L.) shell is an agro-food industrial waste resulting from groundnut processing. With an annual production of over 30 million metric tons of groundnuts globally, a huge amount of groundnut shells is discarded which contains 38-40% cellulose, 15-20% hemicellulose, and 30-35% lignin, showing potential for cellulosic production [6]. Despite their potential, their application in high-quality cellulosic production is still unexplored. Extraction of high-quality cellulosic materials from lignocellulosic materials is challenging, requiring disruption of the strong and rigid matrix of lignin and hemicellulose, which encapsulates the cellulosic materials. Conventional chemical methods have been extensively utilized [7]. Recently, novel approaches such as hydrothermal treatment, microwave extraction, ultrasound extraction, and enzyme extraction have also been explored for the treatment of biomass. Hydrothermal treatment is a process that uses high-temperature water to induce autohydrolysis and delignification [8]. Microwave extraction uses the ability of the biomass to heat internally by the rapid dielectric heating effect [9]. Ultrasound extraction uses the cavitation effect to disrupt the biomass and enhance the penetration of treatment agent. Enzyme extraction uses selective catalysts that can break down non-cellulosic materials under mild reaction conditions [10]. Each of these techniques differs in mechanism, energy requirement, processing time, and effectiveness.

Although these extraction approaches have been individually investigated for various biomass sources, systematic comparative evaluation of multiple extraction techniques for cellulose recovery from groundnut shell biomass remains limited. A direct comparison is essential to determine the most efficient and sustainable method in terms of yield, purity, structural integrity, and physicochemical characteristics. In addition to extraction methodology, particle size of the biomass plays a crucial role in influencing mass transfer, chemical accessibility, and overall extraction efficiency. Therefore, the present study aims at comparative evaluation of hydrothermal, microwave-assisted, ultrasound-assisted, and enzyme-assisted extraction methods for cellulose isolation from groundnut shell biomass using different particle size fractions (300 µm, 450 µm and 600 µm). The combined assessment of process

technique and particle size enables a more comprehensive understanding of their interactive effects on cellulose recovery. The extracted cellulose samples were characterized and benchmarked against commercially available cellulose powder to assess their structural and functional equivalence. This investigation provides insight into the most suitable extraction strategy and optimal particle size for valorizing groundnut shell waste into high-quality cellulose, thereby supporting sustainable biomass utilization and circular bioeconomy development

2. Material and methods

2.1. Materials

Groundnut shells were collected from a local industry at Thanjavur district, Tamil Nadu, India. The chemicals used for the analysis like sodium hydroxide (NaOH), citric acid ($C_6H_8O_7$), sodium chlorite ($NaClO_2$), sodium hypochlorite (Nalo), Hydrogen peroxide (H_2O_2), were purchased from The Precision Scientific Co. (CBE). Commercial cellulose powder was purchased from ISOCHEM.

2.2. Preparation of raw materials

The procured groundnut shells were subjected to washing with distilled water to remove all the dirt and impurities. The washed groundnut shells were then dried in a hot air oven at a temperature of 60 °C for a period of 8 hours. The dried groundnut shells were then powdered using a pulverizer. The powdered form of the groundnut shells was then subjected to sieving using stainless steel mesh sieves of size 300, 450, and 600 µm. The sieving of the powdered form of the groundnut shells was done to assess the effect of particle size on the extraction efficiency of cellulose. The prepared groundnut shells were then stored in airtight containers and kept at room temperature (28 ± 2 °C).

2.3. Extraction of cellulose

Cellulose extraction refers to the isolation of cellulose from lignocellulosic biomass through the systematic removal of non-cellulosic constituents under controlled processing conditions. In the present study, different extraction approaches were employed, including ultrasound, microwave, hydrothermal and enzyme-assisted treatments, each facilitating the disruption of the lignocellulosic matrix through distinct mechanisms.

2.3.1. Ultrasound assisted extraction

Ultrasound assisted extraction of cellulose (USC) from GS powder was carried out according to the method reported by [11], with minor modifications. The biomass powder with distilled water in a solid-to-liquid ratio of 1:10 (w/v) was subjected to US at a frequency of 20 kHz and a power of 100 to 200 W for 10 min at temperature of 60 °C. The mixture was filtered and the residue obtained was mixed with 2N sodium hydroxide solution in the ratio of 1:20 (w/v) and heated for 3h at 80°C with continuous stirring to remove hemicellulose, lignin, etc.,

The mixture was filtered and washed with distilled water until the pH was around neutral. Then delignification was carried out by mixing the biomass with 10% hydrogen peroxide, sodium chlorite and sodium hypochlorite solution in the ratio of 1:20 (w/v), dried weight basis. The pH was maintained at 4 by adding 10% acetic acid and the solution was kept at 80°C/60min with continuous stirring for three cycles. The extracted cellulose was filtered and washed with distilled water until the pH was around neutral. The washed cellulose was dried at 50°C for 12 hours and stored.

2.3.2. Microwave assisted extraction

Microwave assisted extraction of cellulose (MWC)from the GS powder was carried out according to the process reported by [9], with some modifications. The biomass was mixed with distilled water in the ratio of 1:10 (w/v), dried weight basis, and subjected to microwave irradiation at 450 to 630 W for 4 min. The resulting mixture was then processed following the same protocol described in Section 2.3.1.

2.3.3. Hydrothermal assisted extraction

Hydrothermal assisted extraction of cellulose (HTC) was extracted using the method described by [12] with slight modifications. The groundnut shell powder was by first dissolved in distilled water at a ratio of 1:10 (w/v, on dry weight basis) and heated at (60 to 80 °C) for 1 h in a thermostatically controlled water bath. The filtered mixture was then collected for further processing like alkaline treatment followed by bleaching described by USC section.

2.3.4. Enzyme assisted extraction

The enzyme-assisted extraction of cellulose (ENC) from GS powder was carried out according to [10], but the reaction conditions were modified. The biomass was dissolved in distilled water and maintained at a consistency of 5% (w/v), and the pH was adjusted to 4.5 using an acetate buffer solution. The mixture was then treated with laccase enzyme (0.1 to 1.0 mg/g dry biomass) at a temperature of 50°C for a duration of 60 min with continuous agitation. The reaction was then arrested by heating the mixture to 90°C for a duration of 15 min. The mixture was then subjected to filtration and washing with distilled water. The subsequent alkaline and delignification treatments were followed as in section 2.3.1.

2.4. Characterization of extracted cellulose

2.4.1. Component analysis

The Proximate compositions of untreated and treated groundnut shell like pH, ash were analysed using AOAC methods 2001. The chemical composition of was calculated according to the National Renewable Energy Laboratory (NREL) program following the procedure described by [2].

2.4.2. Color analysis

The color analysis of the cellulose samples was carried out with the Hunter Lab Colorimeter ColorFlex EZ (Hunter Associates Laboratory Inc., Virginia, USA), according to the procedure reported by [13]. The total color difference ΔE* was calculated with the Eq. (1)

$$\Delta E = \sqrt{(L - L_0)^2 + (a - a_0)^2 + (b - b_0)^2} \quad (1)$$

2.4.3. Flow properties

The flow properties of the cellulose samples were determined by measuring bulk density and tapped density using a graduated measuring cylinder [9]. The samples of known weight were carefully poured into the graduated measuring cylinder to determine the radius, bulk volume, and the samples were manually tapped to determine the tapped volume. Carr's Index (Eq.2) and Hausner's Ratio (Eq.3) were determined based on the bulk and tapped densities of the samples, and the angle of repose was determined using the fixed funnel method.

$$\text{Carr's index (\%)} = \frac{(\text{Tapped density} - \text{Bulk density})}{\text{Tapped density}} \times 100 \quad (2)$$

$$\text{Hausner's ratio (\%)} = \frac{\text{Tapped density}}{\text{Bulk density}} \quad (3)$$

2.4.4. Solubility

The solubility of cellulose was determined by dissolving 0.2 g of extracted cellulose in 20 mL of 1% (v/v) solution of water & ethanol. The mixture was stirred at 250 rpm for 30 minutes at 25 °C to allow complete interaction between the two components. The mixture was filtered, and the insoluble component was separated by washing with deionized water and then drying to constant weight. The percentage solubility was determined using Eq. (4)

$$\text{Solubility (\%)} = 100 - \frac{\text{Weight of insoluble fraction}}{\text{Initial weight of the sample}} \times 100 \quad (4)$$

2.4.5. Water Holding Capacity (WHC)

Water holding capacity (WHC) was determined using the centrifugation method described by [14] with slight modifications. Briefly, 5 g of cellulose was dispersed in 50 mL of distilled water and homogenized for 1 h at room temperature. The suspension was centrifuged at 5000 × g for 15 min, and the supernatant was discarded. The hydrated residue was weighed, and WHC was calculated following Eq. (5)

$$\text{WHC (g/g)} = 100 - \frac{W_1 - W_0}{W_0} \quad (5)$$

Where, W_0 and W_1 are the weights of the initial and final samples, respectively.

2.4.6. Yield Percentage

The cellulose yield percentage was determined using the following (Eq. 6), as described by [3]

$$\text{Cellulose yield (\%)} = \frac{\text{Weight of cellulose (dry wt, g)}}{\text{Weight of groundnut shell powder (dry wt, g)}} \times 100 \quad (6)$$

where the cellulose yield represents the dried weight of the extracted cellulose, and the initial dry weight corresponds to the bone-dry weight of the starting biomass.

2.4.7. Fourier Transform Infrared Spectroscopy (FTIR)

FTIR was used to identify the functional groups of the cellulose samples. The experiment was carried out according to the method described by [15], and the spectra were recorded with the Fourier transform infrared spectrometer (Shimadzu, USA). The spectral range was set at 4000-400 cm^{-1} with a resolution of 4 cm^{-1}. The results were expressed in percentage transmittance.

2.4.8. Scanning Electron Microscope (SEM)

SEM analysis was done to investigate the surface morphology of the cellulose samples. The micrographs were taken using the scanning electron microscope (Model, Manufacturer, Country), as described by [16]. Before the samples were subjected to the electron microscope, they were sputter-coated with gold to improve their conductivity. Micrographs were taken at an accelerating voltage of 10 kV at suitable magnifications to observe the surface structure.

2.4.9. Differential scanning calorimetry (DSC)

DSC analysis was carried out to assess the thermal properties of cellulose using a DSC 3 STAR system (Mettler Toledo, Zurich, Switzerland). The analysis was carried out according to the method described by [12]. The analysis was carried out on 5 mg of cellulose, which was heated from 30 °C to 450 °C at a rate of 10 °C/min in a nitrogen atmosphere at a rate of 20 mL/min. Onset temperature, degradation temperature, and enthalpy change were determined from the thermogram.

2.4.10. X-ray diffraction (XRD) analysis

X-ray diffraction analysis was performed to investigate the crystallinity of the extracted cellulose. An X-ray diffractometer (Bruker D8 Series) equipped with Cu Kα radiation (λ ~ 1.5406 Å), 40-45 kV, and 20-30 mA was employed for the experiment. The experiment was performed following the procedures reported in [17]. The intensity of the diffracted beam was measured over a 2θ range of 5° to 60°. The crystallinity index and size of the extracted cellulose was calculated by the Segal method using (Eqs.7 & 8), depending on the intensity of the crystalline peak at 22-23°, and the amorphous region at 18-19°.

$$\text{Crystallinity index (CrI, \%)} = (1 - I_{am}/ I_{cry}) \times 100\% \quad (7)$$

Here, I_{am} and I_{cry} represent the amorphous and crystalline peak intensity, respectively

The apparent crystalline size (D) was calculated as described by [18], using Scherrer Eq.7

$$\text{Crystalline size (D, nm)} = K\lambda / \beta\cos\theta \quad (8)$$

Where, K=0.94 (constant), λ represents the wavelength of the X-ray, D and β represent the "apparent crystalline size" and the full length of the diffraction peak measured at half maximum height, respectively.

2.4.11. Particle Size Distribution Analysis

Determination of particle size distribution of the obtained cellulose was carrieed out using a Zetasizer (series Malvern Nano Particle Analyzer, UK). The analysis was performed following the procedure as indicated by [19]. 0.01% Cellulose suspension was prepared in distilled water, and the measurement was done at 25 °C with a refractive index of 1.47. The particle size distribution was recorded based on intensity and all measurements were done in triplicates.

2.4.12. Statistical Analysis

All experiments were conducted in triplicate (n=3), and the mean ± standard deviation (SD) is shown in the tables. The experimental data were analyzed using one-way Analysis of Variance (ANOVA) using SPSS software (version 14.0, SPSS Inc., Illinois, USA). A comparison of means was performed using Turkey's test at a 5% significance level.

3. Results and Discussion

3.1. Optimization of Particle Size for Cellulose Extraction

The particle size is a key factor affecting cellulose extraction efficiency, as it directly controls surface accessibility and mass transfer behaviour. In the current work, 300, 450, and 600µm particle sizes of groundnut

shell were assessed and the maximum cellulose extraction was recorded at 450 µm. This indicates the existence of an optimal particle size threshold rather than a linear relationship between size reduction and yield enhancement. Previous literature has shown that higher recovery of cellulose can be achieved by utilizing smaller sizes. For example, the use of banana pseudo stem with sizes less than or equal to 180 µm showed higher efficiency in the recovery of cellulose during TEMPO-mediated oxidation, which was 25.25% (dry basis), compared to other sizes [20]. Similarly, ultra-fine grinding of lemongrass straw to ≤200 µm was found to improve cellulose recovery, reaching 37.46% using a microwave-assisted alkaline extraction method [9]. Ultra-fine grinding of peanut shell biomass to 200 mesh, or 75 µm, was also found to enable extensive delignification, allowing for 95.2% cellulose purity after sequential chemical treatments [21].

However, in contrast to the results, of the present study showed that further decrease below 300 µm did not proportionally improve the yield. This might be related to the agglomeration of the particles during the pretreatment & alkaline treatment, reduced porosity, and enhanced tendency to lose cellulose during washing and filtration. The low yield obtained in the 600µm can be attributed to inadequate intra-particle diffusions and high chemical accessibility within the biomass structure. The results indicate that the improved performance in the 450µm can be due to the optimum balance between surface area enhancement, structure preservation, yield, and mass transfer efficiency. This result highlights again that cellulose extraction is not solely a matter of maximum size reduction, but of achieving a physicochemical equilibrium where delignification is maximized and damage to the material is minimized.

3.2. Effect of Cellulose Extraction from Groundnut Shell

Extraction of cellulose from the groundnut shell involved pretreatment, alkali treatment, and bleaching to effectively eliminate hemicellulose and lignin from the biomass. Initially, various process intensification methods such as USC, MWC, ENC, and HTC were compared for enhancing the breaking down of the lignocellulosic matrix structure and increasing access to cellulose. Among the HTC conditions, treatment at 70 °C resulted in higher cellulose recovery than 60°C and 80°C due to improved disruption of lignin–hemicellulose interactions without excessive cellulose degradation. Similarly, in MWC, microwave irradiation at 450 W for 4 min showed enhanced cellulose yield compared to 320 W and 540 W treatments due to efficient internal heating and rapid cleavage of ether and ester linkages within the biomass matrix. In the USC method, treatment at 200 W produced comparatively higher cellulose recovery than 150 W and 250 W due to acoustic cavitation, which generated shear forces and microjets capable of disrupting rigid lignin structures and improving reagent penetration into the biomass matrix. Likewise, ENC using laccase at 0.5 mg/g dry biomass demonstrated improved lignin degradation and cellulose accessibility compared to 0.1 and 1.0 mg/g concentrations.

The variation in cellulose yield among the extraction techniques was mainly associated with differences in delignification efficiency and disruption of lignin-carbohydrate complexes (LCCs). MWC yielded the greatest amount of cellulose because of its ability to generate heat quickly and cleave ester and ether links in lignin and hemicellulose [9]. Similarly, USC enhanced cellulose accessibility through cavitation-induced shear forces that disrupted lignin structures and improved reagent penetration into the biomass matrix [22]. ENC promoted selective degradation of amorphous regions under mild processing conditions while preserving cellulose

crystallinity; however, lignin removal efficiency remained lower than energy-assisted treatments [23]. In contrast, HTC showed relatively lower cellulose recovery due to limited disruption of lignin–hemicellulose interactions. The enhanced cellulose recovery observed in MWC and USC treatments could therefore be attributed to improved delignification and greater removal of non-cellulosic components [8].

Post-treatment, the alkaline method, which involved the use of sodium hydroxide (NaOH), to remove hemicellulose by breaking down the ester bonds between the LCC, resulting in the delignification process and the exposure of cellulose [16]. The isolation of the material further progressed through bleaching using hydrogen peroxide (H_2O_2), sodium hypochlorite (NaOCl), and sodium chlorite ($NaOCl_2$). Among them, $NaOCl_2$ showed greater selectivity toward lignin removal while preserving cellulose integrity. After alkaline and $NaOCl_2$ bleaching treatments, cellulose obtained from MWC and USC pretreatments exhibited comparatively higher yield than ENC and HTC methods (Table 1). However, USC was selected as the optimized extraction approach due to its higher cellulose purity, controlled delignification behaviour, and better structural preservation under milder processing conditions compared to MWC.

Table 1 Effect of pre-treatment on yield of extracted cellulose

Particle size (µm)	Extraction method	Cellulose yield (%)
300	USC	36.10±0.58^{b}
	MWC	35.51±0.35^{b}
	HTC	34.00±0.31^{b}
	ENC	32.00±0.83^{b}
450	USC	54.00±1.56^{a}
	MWC	56.75±1.79^{a}
	HTC	50.00±1.58^{a}
	ENC	49.80±0.35^{b}
600	USC	32.52±0.49^{b}
	MWC	34.24±0.34^{b}
	HTC	32.54±0.49^{b}
	ENC	33.27±0.25^{b}

*Data are presented as mean ± SD (n=3). Means with different superscript letters differ significantly ($p < 0.05$), (CC: Commercial cellulose; USC: Ultrasound assisted extraction; MWC: Microwave assisted extraction; ENC: Enzyme assisted extraction; HTC: Hydrothermal assisted extraction)

3.3. Characterization of Extracted Cellulose

3.3.1. Chemical Composition Analysis

The proximate composition of samples is presented in Table 2 analysis was carried out for the optimized 450 µm treated samples selected based on extraction performance. Untreated groundnut shell contained 35.62% α-cellulose, 21.5% hemicellulose, and 29.8% lignin, confirming its lignocellulosic nature and the yield, recovery and loss % of cellulose from groundnut shell at different pretreatment conditions are shown in Table 3. Following pretreatment, a substantial reduction in hemicellulose and lignin content was observed with a corresponding increase in α-cellulose content. Among the treatments, USC exhibited the highest cellulose

enrichment (65.67%), followed by MWC (54.38%), HTC (52.29%), and ENC (49.03%). The reduction of non-cellulosic constituents contributed to improved cellulose purity and enrichment of the crystalline cellulose fraction[24]. The increase in cellulose content after pretreatment indicates effective disruption of lignin–carbohydrate complexes and removal of amorphous non-cellulosic constituents from the biomass structure [25]. Increased cellulose enrichment in USC and MWC pretreatments can be attributed to the efficiency of these pretreatments in eliminating other lignocellulosic components. USC possessed the highest amount of α-cellulose at 65.67%, followed by MWC at 54.38%, while HTC and ENC had low cellulose enrichment. Decreased hemicellulose and lignin contents in the lignocellulosic biomass due to pretreatment could be attributed to effective delignification and elimination of amorphous substances, leading to increased enrichment of cellulose content [17]. The rise in α-cellulose amount relative to the raw groundnut shell is confirms of the effectiveness of the pretreatment and purification methods used in this study. Moreover, the observed differences in composition after the process suggest that the removal of matrix impurities is gradual, thus enhancing the quality of the cellulose extracted. The resource with higher cellulose content might potentially yield a higher quantity of cellulose. However, the utilization of groundnut shell waste played a significant role in this study.

3.3.2. Color

Color is another significant quality attribute of cellulose, and it is an indicator of the effectiveness of delignification and bleaching treatments. Removal of lignin, polyphenol, and other chromophoric compounds during chemical treatment leads to an increase in brightness, measured quantitatively using the CIE L* parameter. An increase in L* indicates an improvement in purity and removal of non-cellulosic components [3]. The lightness (L*) values (Table 4) showed that there are clear differences between the commercial cellulose and the extracted cellulose. The highest lightness was observed for CC - 94.28, which shows a highly purified cellulose with a minimum number of impurities. Amongst the extracted celluloses, USC - 93.31 and ENC - 92.33 have L* values close to the commercial standard, showing a highly effective removal of colored compounds. In comparison, HTC-90.70 and MWC-90.17 exhibited slightly lower values of L* at, indicating a pale-yellow appearance, possibly indicating that further optimization or bleaching may be required to attain a similar level of purity, which is attributed to the presence of minor chromophoric groups [24]. The level of brightness obtained for all the treatments, however, indicates a good level of delignification and improvement in the quality of the cellulose. However, the overall brightness obtained from all treatments proves a successful process in delignification and improvement in quality of cellulose. The differences in colors obtained from treatments also prove the effect of extraction methods in cellulose purification. Significantly, treatments with ultrasound and enzymatic methods resulted in cellulose samples with similar brightness to commercial samples, showing a great potential for cellulose production from agricultural wastes.

Table 2 Chemical composition and properties of raw and treated groundnut shell

Sample	pH	Ash	Moisture Content (%)	Cellulose (%)	Hemicellulose (%)	Lignin (%)
Groundnut shell	5.68 ±0.03^{e}	3.82 ± 0.24^{a}	7.54 ±0.06^{e}	35.62 ± 0.84^{e}	21.5 ± 0.8^{a}	29.8 ± 1.0^{a}
USC	6.08±0.05^{d}	0.40 ± 0.04^{e}	8.68 ±0.08^{d}	65.67 ± 1.45^{a}	6.5 ± 0.5^{e}	7.9 ± 0.6^{e}
MWC	6.89±0.04^{a}	0.68 ± 0.05^{d}	9.56 ±0.07^{c}	54.38 ± 1.32^{b}	7.2 ± 0.6^{c}	9.0 ± 0.7^{c}
ENC	6.48±0.02^{c}	1.12 ± 0.08^{b}	12.22 ±0.10^{a}	52.29 ± 1.26^{c}	8.5 ± 0.7^{b}	8.9 ± 0.8^{d}
HTC	6.72±0.03^{b}	0.94 ± 0.07^{c}	10.32 ±0.06^{b}	49.03 ± 1.18^{d}	7.0 ± 0.6^{d}	10.8 ± 0.9^{b}

*Means followed by different superscript letters within the same Colomn are significantly different at $p < 0.05$ (CC: Commercial cellulose; USC: Ultrasound assisted extraction; MWC: Microwave assisted extraction; ENC: Enzyme assisted extraction; HTC: Hydrothermal assisted extraction)

Table 3 Cellulose yield, recovery, and loss (%) of treated samples

Sample	Cellulose yield (%)	Cellulose recovery (%)	Cellulose loss (%)
USC	54.00 ± 1.56^{b}	35.46 ± 1.24^{a}	64.54^{d}
MWC	56.75 ± 1.79^{a}	30.87 ± 1.16^{b}	69.13^{c}
ENC	49.80 ± 0.35^{c}	26.04 ± 0.92^{c}	73.96^{b}
HTC	50.00 ± 1.58^{c}	24.52 ± 0.88^{d}	75.48^{a}

*Means followed by different superscript letters within the same Colomn are significantly different at $p < 0.05$ (CC: Commercial cellulose; USC: Ultrasound assisted extraction; MWC: Microwave assisted extraction; ENC: Enzyme assisted extraction; HTC: Hydrothermal assisted extraction)

3.3.3. Flow Properties

The flow property is a key property that determines the functional properties of cellulose and its ability to be used as a binder, diluent, and direct compression filler [3]. Table 4 shows the bulk density, tapped density, true density, Carr's index (CI), Hausner ratio (HR), and porosity of the extracted cellulose. The bulk densities of the extracts were found to range between 0.27 g/cm³ and 0.33 g/cm³. USC had the highest bulk density value of 0.332 ± 0.02 g/cm³, which was close to the bulk density value of commercial cellulose. On the other hand, ENC and MWC samples were found to have lower bulk densities of 0.27 g/cm³ and 0.30 g/cm³, respectively. The values for tapped density displayed a similar pattern, indicative of compressibility properties of the cellulose powder. The density of the cellulose, which is an indication of the presence of α-cellulose and purification of non-cellulosic fractions [26]. The increase in the value of true density in some cellulose samples could have been caused by increased crystallinity [27]. Carr's index (CI) is a measure of the compressibility of a powder sample, and its values were recorded to range between 24.55 and 40.0%. However, increased CI values in ENC and MWC powder samples, this shows that the cellulose powder flow behaviour also demonstrate enhanced cohesiveness as a result of fibrous nature and particle interactions [28]. Likewise, Hausner ratio (HR) linked with interparticle friction [12]was between 1.33 to 1.67. USC revealed relatively lower HR values compared to ENC and MWC, which demonstrated higher HR values due to increased particle cohesiveness. The CC powder sample also displayed relatively high HR, reinforcing the poor flowability of the sample. Porosity values of the samples showed an indirect relationship with bulk density values; ENC displayed relatively high porosity values. As described by [10], the porosity, CI, and HR values of commercially available cellulose were 32.08 and 1.47, respectively. Therefore, the overall results indicate that the extraction method significantly influences the particle morphology, packing behaviour, and interparticle interactions of cellulose powders [3]. Among the samples, USC exhibited comparatively lower Carr's index and Hausner ratio values, indicating improved flowability and reduced interparticle friction. In contrast, MWC and ENC showed higher compressibility and cohesiveness, resulting in poor flow behaviour. Thus, ultrasound-assisted extraction produced cellulose with superior flow properties compared to other methods, making it more suitable for applications requiring better powder handling and compressibility.

3.3.4. Solubility

The solubility of cellulose extracted by employing various methods in water and ethanol is showed in Fig.1. The results show a clear variation among the samples, indicating that the extraction process influences the structural organization and intermolecular interactions of cellulose. In the case of water, the maximum solubility was found in HTC 34%, then came USC 33%, MWC 30%, CC 29%, and ENC 29% samples. The reason for the greater solubility in the HTC and USC samples might be associated with the partial destruction of the hydrogen bond structure, making the hydroxyl groups more accessible for water molecules. As for ethanol, the solubility level is much lower for all samples examined, HTC 15% and USC 14% showing slightly higher values compared to others 12-13%. This reaction is mostly dependent on the solvent's polarity. In this regard, water enables swelling and hydrogen bonding, while ethanol has limited ability to penetrate the compact cellulose structure [27]. Solubility variations may be attributed to the differences in crystallinity and amorphous fractions. Amorphous-rich samples are more soluble because of less polymer chain packing and weak intermolecular forces [26].

Crystalline samples are less soluble because of hindrance from solvent penetration. Overall, the solubility of HTC and USC samples is better because of disintegrated structures in extraction processes.

3.3.5. Water Holding Capacity (WHC)

The water holding capacity (WHC) of cellulose is an essential functional attribute that defines the ability of cellulose to absorb and retain water within its structure [29]. The WHC result of the extracted cellulose sample are shown in Table 4. When compared with the CC similar result reported in[14], USC (9.81± 0.08) exhibited higher WHC, which may be attributed to the disruption of the compact lignocellulosic matrix and increased accessibility of hydrophilic groups during ultrasonic treatment. Similarly, MWC also had considerable WHC because of structural modification and enhanced fiber swelling[30]. However, HTC and ENC exhibited relatively lower values of WHC compared to USC and MWC due to the structural alteration and increased crystallinity, which made water binding sites less available[31]. The differences in WHC values observed in these samples are an indication that the various extraction and treatments applied have greatly influenced the microstructure, porosity, and surface properties of cellulose[32]. Amorphous cellulose materials have relatively high-water binding capacity since their polymer chains are readily available for interaction with water molecules. Previous research findings indicated that changes in crystallinity and amorphous nature greatly influence WHC values[29].

Table 4 Color, WHC and flow properties of extracted cellulose and commercial cellulose

Sample	WHC (g/g)	Color ΔE	Bulk density (g/cm³)	Tapped density (g/cm³)	True density (g/cm³)	Carr's index (CI, %)	Hausner's ratio (HR)	Porosity
CC	3.21 ± 0.05^{b}	–	0.290 ± 0.01^{c}	0.427 ± 0.02^{b}	1.380 ± 0.08^{d}	32.08 ± 2.80^{b}	1.47 ± 0.07^{b}	0.790 ± 0.02^{b}
USC	9.81 ± 0.08^{a}	3.53 ± 0.10^{c}	0.332 ± 0.02^{a}	0.440 ± 0.02^{b}	1.490 ± 0.09^{a}	24.55 ± 2.50^{d}	1.33 ± 0.06^{c}	0.792 ± 0.02^{b}
HTC	9.58 ± 0.09^{a}	6.60 ± 0.15^{a}	0.310 ± 0.02^{b}	0.420 ± 0.02^{b}	1.480 ± 0.10^{a}	26.19 ± 2.30^{c}	1.35 ± 0.05^{c}	0.790 ± 0.02^{b}
ENC	9.25 ± 0.08^{a}	4.71 ± 0.12^{b}	0.270 ± 0.01^{d}	0.400 ± 0.02^{c}	1.440 ± 0.09^{c}	32.50 ± 2.70^{b}	1.48 ± 0.07^{b}	0.812 ± 0.02^{a}
MWC	9.12 ± 0.07^{a}	6.95 ± 0.18^{a}	0.300 ± 0.02^{b}	0.500 ± 0.03^{a}	1.460 ± 0.10^{b}	40.00 ± 3.20^{a}	1.67 ± 0.10^{a}	0.795 ± 0.02^{b}

*Means followed by different superscript letters within the same Colomn are significantly different at $p < 0.05$ (CC: Commercial cellulose; USC: Ultrasound assisted extraction; MWC: Microwave assisted extraction; ENC: Enzyme assisted extraction; HTC: Hydrothermal assisted extraction)

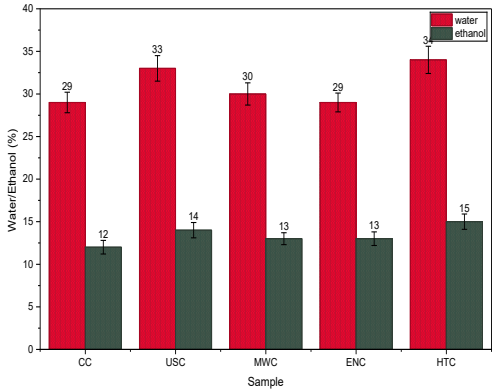


Fig.1 Solubility of Cellulose

3.3.6. Fourier Transform Infrared Spectroscopy

FTIR Spectroscopy was performed to compare the structures of cellulose extracted using various process intensification techniques compared with commercial cellulose, as shown in Fig.2. The commercial cellulose had characteristic peaks for cellulose, such as a broad peak representing O-H stretching at about 3342 cm^{-1} and a C-H stretching peak at about 2893 cm^{-1}, and similar peaks were seen in the extracted samples, showing that the backbone structure of the cellulose was preserved. Which, indicating that no significant chemical modification occurred during pretreatment [12]. The absorption peak observed at 1734 cm^{-1}, which is indicative of the stretching vibration of C=O bonds of acetyl or ester groups present in hemicellulose, was evident in some samples treated with acid and water compared to the commercial cellulose sample, which indicates the presence of non-cellulosic materials [14]. Nevertheless, the low intensity of the peak showed that there has been a significant loss of hemicellulose from the biomass samples. Likewise, the vibration peak observed at 1527 cm^{-1}, which represents the vibration of the aromatic compounds present in lignin, is low for the commercial cellulose sample and considerably lower for USC and ENC samples [17]. In addition, the peak that existed around 1028 cm^{-1} representing C-O-C and the β-1,4-glycosidic bond was almost constant in all samples of cellulose. In summary, the high similarity of IR profiles of extracted and commercial cellulose clearly shows the efficiency of pretreatments carried out in this work for obtaining cellulose of comparable structure, although with slight deviations due to the effectiveness of purification processes and hydrogen bonds, among other factors. This finding is consistent with findings from previous literature [33]. Overall, the FTIR results indicate that USC exhibited spectra most closely resembling that of commercial cellulose, with reduced intensities of hemicellulose and lignin associated peaks. This suggests more effective removal of non-cellulosic components and better purification efficiency. In contrast, other samples showed relatively higher residual peaks, indicating incomplete delignification. Therefore, ultrasound-assisted extraction yielded cellulose with comparatively higher structural purity among the investigated methods.

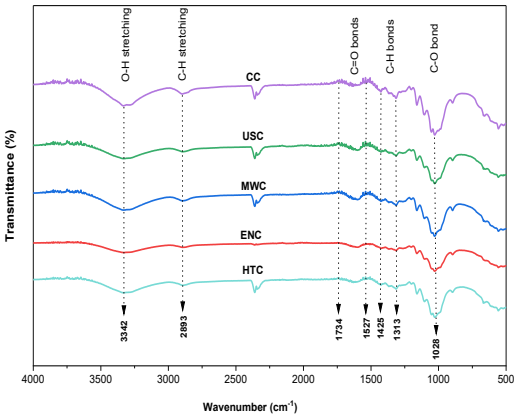


Fig.2 FTIR spectra of cellulose

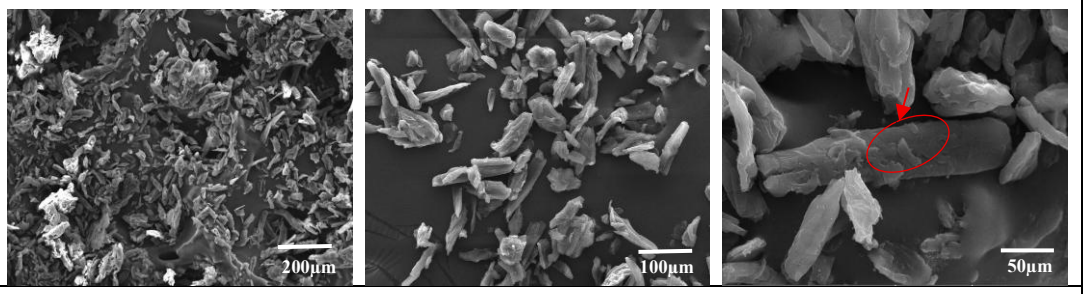
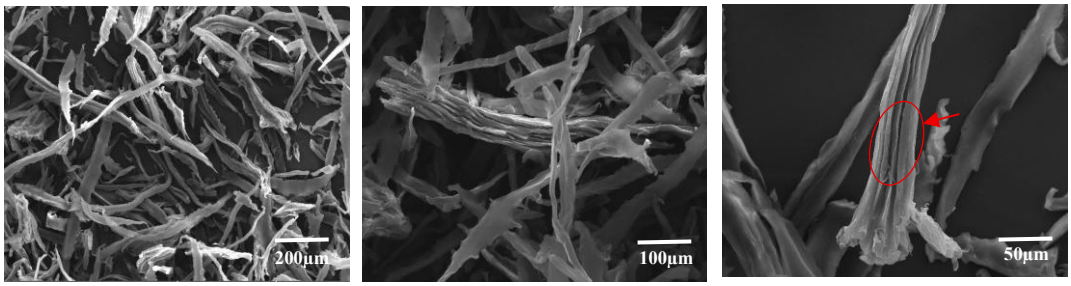
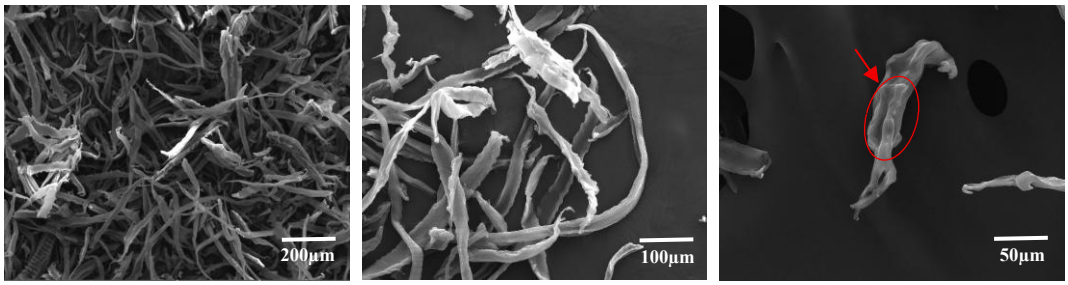
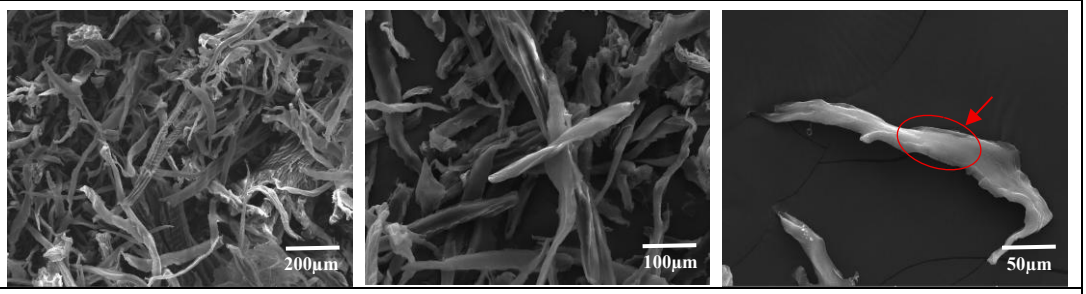
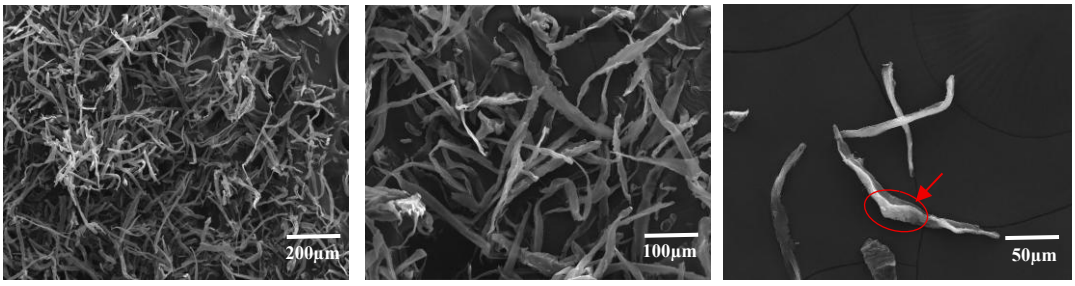
3.3.7. Scanning Electron Microscopy

The structural features of commercial cellulose and extracted cellulose by employing various pretreatment methods were analyzed through scanning electron microscopy (SEM) for assessing the effect of the cellulose isolation method on fiber morphology (Table 4). The SEM images captured at magnifications ranging from 100× to 1000× showed distinct differences in terms of particle morphology, fiber organization, and surface morphology between the samples. CC possessed tight clusters made up of irregular pieces and rod-shaped particles, suggesting a denser morphology with little fibrillation. This tight cluster formation is usually observed in commercially prepared cellulose, wherein particle clustering might take place during drying and grinding procedures. On the other hand, cellulose produced following pretreatment exhibited loosely structured and fibrillated characteristics, implying efficient disintegration of the lignocellulosic structure and removal of non-cellulosic elements. Cellulose obtained USC technique possessed a more elongated and entangled fibril structure with partially separated microfibrils to form a porous heterogeneous network. Such structural modifications could be related to cavitation effects induced by ultrasonic waves, such mechanical effects make it easier to strip away the amorphous phases like lignin and hemicellulose, thus leading to exposure of cellulose microfibrils and formation of an isolated fibrous structure without altering the crystalline cellulose regions, as previously observed [24].

The cellulose that was obtained from MWC showed fragmented fibrous structures where the microfibers were curled and partially decomposed. The quick rise in volumetric temperature caused by microwaves could produce pressure in the biomass matrix, causing a breakdown in the lignin-carbohydrate bond. In this case, the rigid and compact structure of lignocelluloses will break down, producing a fragmented cellulose structure. Fibrous-like structure consisting of elongated and relatively smooth fibrils has been reported to be present in cellulose extracted from cornhusk and wheat straw [24].

Cellulose from ENC yielded comparatively smoother fibrous structures where some of the microfibers appeared to be partially separated. Enzyme-mediated degradation only affected the amorphous polysaccharide portion of the structure, i.e., hemicellulose, leading to isolated cellulose microfibrils without any disruption[34]. Unlike this, cellulose generated using HTC possessed thin and elongated fibers, some being partially broken apart, thus creating a loosely packed fibrous structure. The hydrothermal treatment technique initiates autohydrolysis reaction, breaking down lignin-carbohydrate bonds and thus separating the fibers from the biomass. Altogether, the SEM results indicate that the pretreatment methods employed have significantly altered the cellulose morphology, thus making the cellulose structure more fibrillated and separated from each other. The alterations in the cellulose morphology show the importance of the pretreatment methods in affecting the structural properties of cellulose. The SEM analysis revealed that USC exhibited a more fibrillated, porous, and well-separated microfibrillar structure compared to other samples, indicating effective disruption of the lignocellulosic matrix. The enhanced fibrillation and reduced aggregation suggest efficient removal of amorphous components such as lignin and hemicellulose. In contrast, MWC, ENC, and HTC samples showed comparatively less uniform and partially aggregated structures. Therefore, USC produced cellulose with superior morphological characteristics and better fiber individualization among the investigated methods.

Table 4 SEM micrographs of cellulose

Extraction Techniques	Scanning Electron Microscope Image
CC	
USC	
MWC	
ENC	
HTC	

*CC: Commercial cellulose; USC: Ultrasound assisted extraction; MWC: Microwave assisted extraction; ENC: Enzyme assisted extraction; HTC: Hydrothermal assisted extraction, respectively

3.3.8. Differential Scanning Calorimetry

Thermal behaviour is an important parameter for evaluating the application potential of extracted cellulose obtained through different extraction methods and was analysed using DSC as shown in Fig.3. Different peaks were seen in the thermogram indicating the thermal events involved with the loss of moisture and decomposition of the cellulose samples as well as the non-cellulosic content. An initial broad peak is noticed in the range of 80-120 °C for all samples. This can be due to the loss of water that is physically absorbed by cellulose in the form of hydroxyl groups. The difference in peak intensity among samples indicates differences in moisture, surface property, and porosity formed from different extraction processes [14]. The second thermal transition was observed in the temperature range of 160-220 °C, which reflects the thermal degradation of amorphous phases, mostly due to the residual presence of hemicelluloses and low-molecular compounds. Samples obtained from HTC and ENC treatments had broader and stronger peaks in this temperature range, implying greater amorphous content along with the inability to remove all the non-cellulosic compounds. On the contrary, MWC and USC samples demonstrated weaker peaks in the same temperature range, showing that amorphous structures were successfully removed and refined [12]. The main endothermic degradation peak, which can be found in the range of 280-360 °C, refers to the degradation of the cellulose chain by breaking the β-1,4 glycosidic bonds. This stage marks the first thermal degradation of cellulose and is indicative of the amount of energy needed to disrupt hydrogen bonding between molecules in the polymer. The shift of the peak to higher temperatures denotes enhanced thermal stability, which correlates with greater crystallization and structural organization [35]. The shift in the temperature of degradation peaks to higher temperatures is usually linked to higher crystallinity and hydrogen bonding between cellulose molecules. Lignin and hemicellulose are effectively removed during chemical modification; thus, there are fewer amorphous structures in cellulose, and its molecular structure becomes more organized. On the other hand, HTC and ENC exhibit low temperatures for degradation, which denote the presence of lignin and hemicellulose. Generally, the thermal stability of the samples occurred in the following order: CC > MWC > USC > ENC > HTC (Table 5), and this result is highly consistent with the level of purification and ordering in the process of extraction, especially use of MWC and USC, were better in terms of the thermal stability of cellulose. These observations are very significant to the potential use of the isolated cellulose in high-temperature applications.

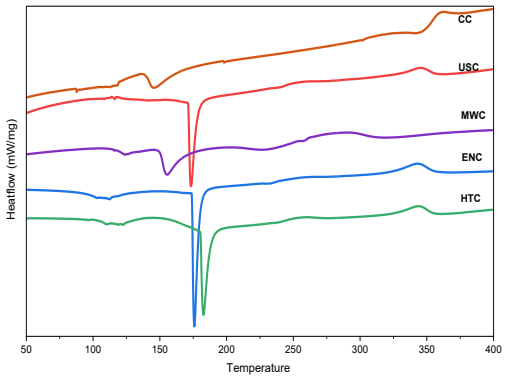


Fig.3 DSC thermogram of cellulose

Table 5 Thermal properties of cellulose obtained from DSC

Sample	To (°C)	Te (°C)	Td (°C)
CC	136	158	145
USC	173	175	186
MWC	148	155	176
ENC	170	173	182
HTC	180	182	192

*CC: Commercial cellulose; USC: Ultrasound assisted extraction; MWC: Microwave assisted extraction; ENC: Enzyme assisted extraction; HTC: Hydrothermal assisted extraction, respectively

3.3.9. X-Ray Diffraction

The crystallinity of cellulose fibers was measured using x-ray diffraction analysis. The purity of cellulose fibers determines their crystallinity. Commercial cellulose and extracted cellulose fiber were used and analysed for crystallinity. Fig.4. shows both types of cellulose fibers show sharp peaks at angles of 2θ = 15° - 16°, 22° - 23°, and 34° - 35°, which represent (1-10)/(110), (200), and (004) crystallographic planes of cellulose I, respectively. The pattern is quite similar to the results obtained from the pretreated lignocellulosic biomass that showed peaks due to cellulose I [17]. Cellulose crystals are formed due to hydrogen bonds within and between cellulose molecules, in addition to van der Waals forces between cellulose molecules, leading to a well-ordered structure. However, lignin and hemicellulose do not have such characteristics since they are mainly amorphous in nature. Therefore, the presence of lignin and hemicellulose decreases the relative crystallinity of cellulose after pretreatment [36]. It is evident from the differences in peak intensity and sharpness observed in the different samples. The CC sample had high peak intensities and sharpness, which suggest that cellulose had a highly ordered crystalline structure devoid of amorphous structures [37]. This is because there is proper disruption of the lignocellulosic structure, thus removal of amorphous materials, leading to more effective packing of cellulose chains with strong hydrogen bonding[24]. USC treatments normally remove the amorphous materials, leading to high crystallinity of cellulose. However, the ENC sample exhibited broad and weak peaks, meaning that the crystallinity level was relatively low. This might have been due to the specificity of the enzyme action only the lignin without affecting the crystalline parts of the cellulose, hence retaining some of the amorphous parts. Similarly, the peaks obtained from the HTC sample were weak and broad, showing that there was partial breakdown of the crystalline regions of the cellulose[8]. The crystallite size also correlated with CrI, the crystalline size of extracted cellulose & commercial cellulose is shown in Table 6. Preservation of the cellulose I form in all samples demonstrates the applicability of the processes for cellulose extraction. USC treated samples exhibited higher crystallinity indices and sharper diffraction peaks, indicating more ordered cellulose structure due to effective removal of amorphous components. The increased crystallite size further confirms improved structural organization and strong intermolecular hydrogen bonding. In contrast, remining three showed significantly lower crystallinity, reflecting incomplete removal of non-cellulosic materials. Therefore, microwave and ultrasound-assisted extractions produced cellulose with superior crystalline characteristics among the investigated methods.

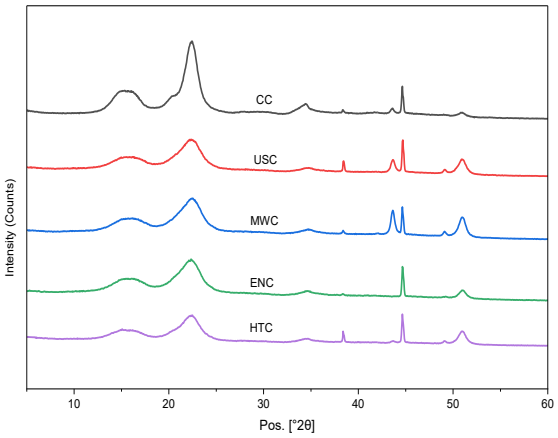


Fig.4 XRD diffractogram of cellulose

Table 6 Crystallinity index and crystalline size of cellulose

Sample	Crystallinity index (Crl, %)	Average crystallite size (D, µm)
CC	68.31	3.4
USC	73.44	4.1
MWC	71.88	3.8
ENC	72.03	3.9
HTC	47.87	2.3

*CC: Commercial cellulose; USC: Ultrasound assisted extraction; MWC: Microwave assisted extraction; ENC: Enzyme assisted extraction; HTC: Hydrothermal assisted extraction, respectively

3.3.10. Particle Size Distribution Analysis

The particles' sizes distribution profiles of CC and extracted cellulose through various process intensification techniques have been shown in Fig. 5(a-e). Particle size is one of the significant factors affecting the dispersion properties, surface characteristics, and structural homogeneity of cellulose. The average particle sizes of CC, USC, MWC, HTC, and ENC are 509.1, 183.5, 496.6, 308.8, and 722.3 d. nm, respectively. The variations in particle sizes suggest that there was a considerable impact of the pretreatment techniques on the disintegration and fibrillation behaviours of the isolated cellulose. Among the several pretreatments applied, the USC method had the lowest particle size of 183.5 d. nm, which indicates effective disintegration of the lignocellulosic structure and breaking of cellulose fibers. The reduction in particle size may be associated with effective removal of lignin, hemicellulose, and other amorphous constituents during pretreatment and purification processes, resulting in improved cellulose refinement. A similar study was conducted by [38], wherein the removal of non-cellulosic compounds facilitated the reduction in particle size and increased the homogeneity of cellulose structure formation. The HTC showed a relatively low particle size of 308.8 d. nm, suggesting that there were only slight structural degradation and cellulose fibrillation due to the process. On the other hand, the highest particle size was seen in the ENC (722.3 d. nm) and MWC (496.6 d. nm). Large-sized particles can be associated with the incomplete fragmentation of cellulose bundles, along with the fibrils remaining connected post-treatment. Previous studies on cellulose recovered from agricultural waste under varying pretreatments exhibited similar results in terms of wide ranges in sizes and their aggregation behaviour [19]. Moreover, larger sized

particles found in ENC could also be due to the mild process of enzyme treatment where only amorphous areas are cleaved off while fibrils remain intact. Commercial cellulose showed comparatively broader distribution of particle size compared to USC-treated cellulose, whereas USC demonstrated improved particle refinement and dispersion characteristics. Particle size distribution curves also indicated that there is multimodal distribution of particles, showing that smaller cellulose particles exist in combination with bigger aggregating particles. Multimodal distribution for cellulose and nanocellulose materials has been reported in literature because of heterogeneous fibrillation and particle agglomeration processes[24]. Overall, among the investigated treatments, USC demonstrated superior particle size reduction and improved distribution characteristics, indicating its effectiveness in producing structurally refined cellulose.

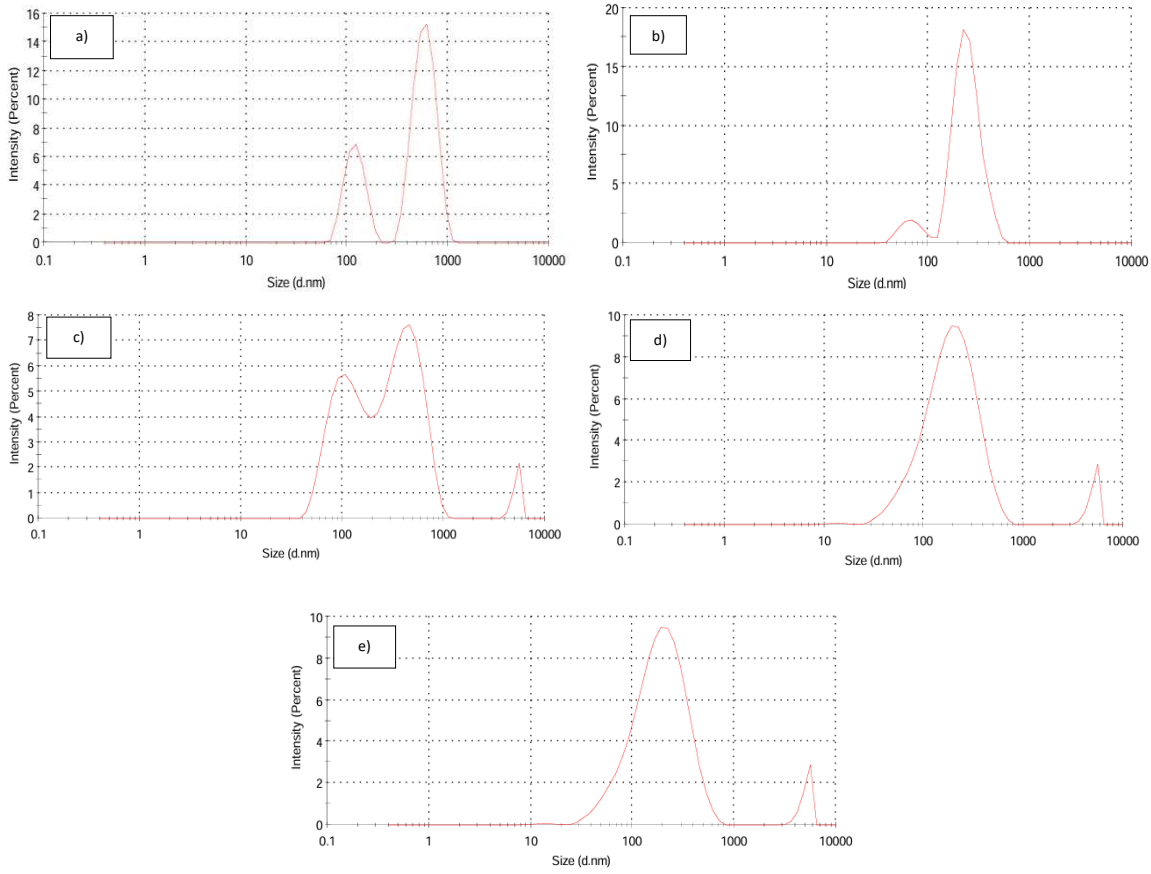


Fig.5 Particle Size Distribution a) CC, b) USC, c) MWC, d) HTC, e) ENC

4. Conclusion

The present study demonstrated the efficient valorization of groundnut shell waste as a sustainable source for cellulose production through the combined influence of process intensification techniques and particle size optimization. Among the selected particle sizes, 450 µm was found to be optimal, providing a balance between mass transfer efficiency and structural integrity, resulting in higher cellulose recovery up to 56.75%. Among the extraction techniques, MWC showed the highest cellulose yield due to effective disruption of the lignocellulosic matrix, while USC resulted in comparatively higher purity, better fibrillated morphology, and improved flow properties. In contrast, ENC and HTC exhibited relatively lower efficiency in terms of yield, structural

refinement and particle size distribution. Characterization results confirmed the preservation of cellulose I structure across all treatments, along with significant removal of lignin and hemicellulose, leading to increased α-cellulose content, enhanced crystallinity, and improved thermal stability. Furthermore, the extracted cellulose exhibited physicochemical properties comparable to CC, including color, solubility, and functional performance, highlighting its potential as a sustainable and cost-effective alternative. Although MWC achieved higher yield, USC demonstrated superior overall performance in terms of purity, structural integrity, and morphology. Therefore, USC can be considered the most suitable method for producing high-quality cellulose from groundnut shell for advanced food, pharmaceutical, and biodegradable applications.

Acknowledgments: The authors thank the Ministry of Food Processing Industries (MoFPI), Government of India, for financial support and NIFTEM-Thanjavur for providing the necessary laboratory facilities and infrastructure support for this research.

Author Contribution: Santhosh K: methodology design, conducting the experiment, acquisition, analysis, interpretation of data, and writing the original draft. Dashelya K: conducting the experiment and acquisition of data. Pratibha Singh: review and editing of the draft. R. Vidyalakshmi: review and editing of the draft. Sinija V. R.: conceptualization, methodology design, review and editing of the draft, supervision, and project administration.

Data availability: The manuscript has no associated data.

Declarations

Ethical approval Not applicable.

Consent to participate Not applicable.

Conflict of interest The authors declare no competing interests

References

1. Riseh RS, Vazvani MG, Hassanisaadi M, Thakur VK (2024) Agricultural wastes: A practical and potential source for the isolation and preparation of cellulose and application in agriculture and different industries. Ind Crops Prod 208:117904. https://doi.org/10.1016/j.indcrop.2023.117904

2. Lu A, Yu X, Ji Q, et al (2023) Preparation and characterization of lignin-containing cellulose nanocrystals from peanut shells using a deep eutectic solvent containing lignin-derived phenol. Ind Crops Prod 195:116415. https://doi.org/10.1016/j.indcrop.2023.116415

3. Buvaneswaran M, Gopan A, V. R. S (2025) Extraction and characterization of methylcellulose from pineapple processing industry waste. Biomass Convers Biorefinery 15:29121–29134. https://doi.org/10.1007/s13399-025-06520-w

4. Al kamzari SMA, Nageswara Rao L, Lakavat M, et al (2023) Extraction and characterization of cellulose from agricultural waste materials. Mater Today Proc 80:2740–2743. https://doi.org/10.1016/j.matpr.2021.07.030

5. Abolore RS, Jaiswal S, Jaiswal AK (2024) Green and sustainable pretreatment methods for cellulose extraction from lignocellulosic biomass and its applications: A review. Carbohydr Polym Technol Appl 7:100396. https://doi.org/10.1016/j.carpta.2023.100396

6. Ganguly P, Sengupta S, Das P, Bhowal A (2020) Valorization of food waste: Extraction of cellulose, lignin and their application in energy use and water treatment. Fuel 280:118581. https://doi.org/10.1016/j.fuel.2020.118581

7. García-Mahecha M, Soto-Valdez H, Peralta E, et al (2023) Production and Characterization of Cellulosic Pulp from Mango Agro-Industrial Waste and Potential Applications. Polymers (Basel) 15:3163. https://doi.org/10.3390/polym15153163

8. Jaturapiree A, Saowapark T, Sukrat K, Chaichana E (2025) Hydrothermal Extraction of Cellulose from Sugarcane Bagasse for Production of Biodegradable Food Containers. Recycling 10:110. https://doi.org/10.3390/recycling10030110

9. Bahndral A, Shams R, Dash KK, et al (2024) Microwave assisted extraction of cellulose from lemon grass: Effect on techno-functional and microstructural properties. J Agric Food Res 16:101170. https://doi.org/10.1016/j.jafr.2024.101170

10. Li J, Zhang S, Li H, et al (2018) Cellulase pretreatment for enhancing cold caustic extraction-based separation of hemicelluloses and cellulose from cellulosic fibers. Bioresour Technol 251:1–6. https://doi.org/10.1016/j.biortech.2017.12.026

11. Freitas PAV, González-Martínez C, Chiralt A (2022) Applying ultrasound-assisted processing to obtain cellulose fibres from rice straw to be used as reinforcing agents. Innov Food Sci Emerg Technol 76:102932. https://doi.org/10.1016/j.ifset.2022.102932

12. Harini U, Harish S, Harishankar A, et al (2024) Extraction and characterization of microcrystalline cellulose from wine waste. Food Bioprod Process 144:92–101. https://doi.org/10.1016/j.fbp.2024.01.001

13. Harish S, Sandhya K, Hema V, et al (2025) Comparative evaluation of pulsed electric field and assisted technology alkalization on the quality characteristics of cocoa powder. Innov Food Sci Emerg Technol 106:104245. https://doi.org/10.1016/j.ifset.2025.104245

14. Brahma R, Ray S (2024) Optimization of extraction conditions for cellulose from jackfruit peel using RSM, its characterization and comparative studies to commercial cellulose. Meas Food 13:100130. https://doi.org/10.1016/j.meafoo.2023.100130

15. Hafid HS, Omar FN, Zhu J, Wakisaka M (2021) Enhanced crystallinity and thermal properties of cellulose from rice husk using acid hydrolysis treatment. Carbohydr Polym 260:117789. https://doi.org/10.1016/j.carbpol.2021.117789

16. Moghaddam MK, Gheshlagh FG, Moezzi M (2024) Extraction and characterization of cellulose microfibers from cornhusk for application as reinforcing agent in biocomposite. Int J Biol Macromol 264:130669. https://doi.org/10.1016/j.ijbiomac.2024.130669

17. Sunesh NP, Suyambulingam I, Divakaran D, et al (2025) Isolation and characterization of cellulose particles from groundnut (Arachis hypogaea) shell waste for sustainable reinforcement applications. Int J Biol Macromol 327:147228. https://doi.org/10.1016/j.ijbiomac.2025.147228

18. Varghese SM, Bhosale YK, Aruna Nair UK, et al (2022) Valorisation and Characterization of Allium cepa var. aggregatum Biowastes for the Production of Microcrystalline Cellulose. Waste and Biomass Valorization 13:1931–1944. https://doi.org/10.1007/s12649-021-01625-5

19. Chumchoochart W, Ketvaraporn T, Chandet N, et al (2025) Granular nanocellulose derived from sugarcane bagasse and corn stover: Production, characterization, and its potential for lipid hydrolysis reduction. Carbohydr Polym Technol Appl 10:100851. https://doi.org/10.1016/j.carpta.2025.100851

20. Nascimento REA, Carvalheira M, Crespo JG, Neves LA (2023) Extraction and Characterization of Cellulose Obtained from Banana Plant Pseudostem. Clean Technol 5:1028–1043. https://doi.org/10.3390/cleantechnol5030052

21. Chen K, Wang L, Xu L, et al (2023) Preparation of peanut shell cellulose nanofibrils and their superhydrophobic aerogels and their application on cotton fabrics. J Porous Mater 30:471–483. https://doi.org/10.1007/s10934-022-01354-7

22. EL KHAYAT DRIAA Y, MAARIR H, MENNANI M, et al (2025) Ultrasound, pulsed electric fields, and high-voltage electrical discharges assisted extraction of cellulose and lignin from walnut shells. Int J Biol Macromol 292:139319. https://doi.org/10.1016/j.ijbiomac.2024.139319

23. Kijpornyongpan T, Schwartz A, Yaguchi A, Salvachúa D (2022) Systems biology-guided understanding of white-rot fungi for biotechnological applications: A review. iScience 25:104640. https://doi.org/10.1016/j.isci.2022.104640

24. Wardani RK, Holilah H, Bahruji H, et al (2024) The comparison of hydrothermal, ultrasonication and microwave assisted alkalization of cellulose from Borassus flabellifer fruit husk. Sustain Chem Pharm 39:101583. https://doi.org/10.1016/j.scp.2024.101583

25. Devarajan MM, Kumaraguruparan G, Nagarajan KJ, Vignesh C (2024) Production of hybrid AgNPs - TEMPO-mediated oxidation cellulose composite from jackfruit peduncle agro-waste and its thermal management application in electronic devices. Int J Biol Macromol 254:127848. https://doi.org/10.1016/j.ijbiomac.2023.127848

26. Adeleye OA, Bamiro OA, Albalawi DA, et al (2022) Characterizations of Alpha-Cellulose and Microcrystalline Cellulose Isolated from Cocoa Pod Husk as a Potential Pharmaceutical Excipient. Materials (Basel) 15:5992. https://doi.org/10.3390/ma15175992

27. Ejikeme PM (2008) Investigation of the physicochemical properties of microcrystalline cellulose from agricultural wastes I: orange mesocarp. Cellulose 15:141–147. https://doi.org/10.1007/s10570-007-9147-7

28. Tasnim S, Tipu MFK, Rana MS, et al (2023) Modification of Bulk Density, Flow Property and Crystallinity of Microcrystalline Cellulose Prepared from Waste Cotton. Materials (Basel) 16:5664. https://doi.org/10.3390/ma16165664

29. Raclavská H, Šafář M, Raclavský K, et al (2025) Use of Cellulose from Waste Paper to Improve the Water Capacity of Soils Within the Circular Economy. Agriculture 15:1880. https://doi.org/10.3390/agriculture15171880

30. Nishimura A, Otsuka S (2024) Sulfated cellulose pulp with high water retention and a swollen fiber structure for the preparation of completely dispersed cellulose nanofibers. Cellulose 31:3561–3571. https://doi.org/10.1007/s10570-024-05841-9

31. Xiao Y, Liu Y, Wang X, et al (2019) Cellulose nanocrystals prepared from wheat bran: Characterization and cytotoxicity assessment. Int J Biol Macromol 140:225–233. https://doi.org/10.1016/j.ijbiomac.2019.08.160

32. Agarwal UP (2022) Beyond Crystallinity: Using Raman Spectroscopic Methods to Further Define Aggregated/Supramolecular Structure of Cellulose. Front Energy Res 10:. https://doi.org/10.3389/fenrg.2022.857621

33. Klaai L, Hammiche D, Boukerrou A, Pandit V (2022) Thermal and structural analyses of extracted cellulose from olive husk. Mater Today Proc 52:104–107. https://doi.org/10.1016/j.matpr.2021.10.498

34. Signori-Iamin G, Marquez R, Bastida GA, et al (2026) Enzyme-assisted high-consistency fiber refining: enhancing cellulose materials performance in the paper industry through process and physics-informed machine learning modeling. Cellulose 33:1595–1615. https://doi.org/10.1007/s10570-025-06921-0

35. Vallejo M, Cordeiro R, Dias PAN, et al (2021) Recovery and evaluation of cellulose from agroindustrial residues of corn, grape, pomegranate, strawberry-tree fruit and fava. Bioresour Bioprocess 8:25. https://doi.org/10.1186/s40643-021-00377-3

36. Salaenoi J, Jurejan N, Yokthongwattana C, et al (2024) Characteristics of coconut husk cellulose and its effectiveness as a potassium permanganate absorbent for fishery applications. Case Stud Chem Environ Eng 10:100975. https://doi.org/10.1016/j.cscee.2024.100975

37. Balasubramani V, Nagarajan KJ, Karthic M, Pandiyarajan R (2024) Extraction of lignocellulosic fiber and cellulose microfibrils from agro waste-palmyra fruit peduncle: Water retting, chlorine-free chemical treatments, physio-chemical, morphological, and thermal characterization. Int J Biol Macromol 259:129273. https://doi.org/10.1016/j.ijbiomac.2024.129273

38. Pattnaik F, Nanda S, Kumar V, et al (2022) Isolation of cellulose fibers from wetland reed grass through an integrated subcritical water hydrolysis-pulping-bleaching process. Fuel 311:122618. https://doi.org/10.1016/j.fuel.2021.122618